JACS
JOURNAL OF THE AMERICAN CHEMICAL SOCIETY
Communication
pubs.acs.org/JACS

Structure of Chiral $Au_{44}(2,4\text{-DMBT})_{26}$ Nanocluster with an 18-Electron Shell Closure

Lingwen Liao,[†,∥] Shengli Zhuang,[†,∥] Chuanhao Yao,[†] Nan Yan,[†] Jishi Chen,[†] Chengming Wang,[‡] Nan Xia,[†] Xu Liu,[†] Man-Bo Li,[†] Lingling Li,[§] Xiaoli Bao,[§] and Zhikun Wu*[,†]

[†]Key Laboratory of Materials Physics, Anhui Key Laboratory of Nanomaterials and Nanotechnology, Institute of Solid State Physics, Chinese Academy of Sciences, Hefei, Anhui 230031, China

[‡]Hefei National Laboratory for Physical Sciences at the Microscale, University of Science and Technology of China, Hefei, Anhui 230026, China

[§]Instrumental Analysis Center, Shanghai Jiaotong University, Shanghai 200240, China

Supporting Information

ABSTRACT: The 18-electron shell closure structure of Au nanoclusters protected by thiol ligands has not been reported until now. Herein, we synthesize a novel nanocluster bearing the same gold atom number but a different thiolate number as another structurally resolved nanocluster $Au_{44}(TBBT)_{28}$ (TBBTH = 4-*tert*-butylbenzenelthiol). The new cluster was determined to be $Au_{44}(2,4\text{-DMBT})_{26}$ (2,4-DMBTH = 2,4-dimethylbenzenethiol) using multiple techniques, including mass spectrometry and single crystal X-ray crystallography (SCXC). $Au_{44}(2,4\text{-DMBT})_{26}$ represents the first 18-electron closed-shell gold nanocluster. SCXC reveals that the atomic structure of $Au_{44}(2,4\text{-DMBT})_{26}$ is completely different from that of $Au_{44}(TBBT)_{28}$ but is similar to the structure of Au_{38Q}. The arrangement of staples (bridging thiolates) and part of the Au_{29} kernel atom induces the chirality of $Au_{44}(2,4\text{-DMBT})_{26}$. The finding that a small portion of the gold kernel exhibits chirality is interesting because it has not been previously reported to the best of our knowledge. Although $Au_{44}(2,4\text{-DMBT})_{26}$ bears an 18-electron shell closure structure, it is less thermostable than $Au_{44}(TBBT)_{28}$, indicating that multiple factors contribute to the thermostability of gold nanoclusters. Surprisingly, the small difference in Au/thiolate molar ratio between $Au_{44}(2,4\text{-DMBT})_{26}$ and $Au_{44}(TBBT)_{28}$ leads to a dramatic distinction in Au 4f X-ray photoelectron spectroscopy, where it is found that the charge state of Au in $Au_{44}(2,4\text{-DMBT})_{26}$ is remarkably more positive than that in $Au_{44}(TBBT)_{28}$ and even slightly more positive than the charge states of gold in Au-(2,4-DMBT) or Au-TBBT complexes.

Breakthroughs have recently been achieved in gold nanocluster research, and a series of gold nanoclusters have been synthesized and structurally resolved.[1] However, our understanding of the compositions and structures of the nanoclusters is far from complete. For instance, the superatom concept was employed to successfully interpret the stability of Au_{25} nanoclusters, whereas this concept cannot be employed to predict nanocluster composition.[1a,2] Even the stable 18-electron closed-shell structure of thiolated gold nanoclusters has not been experimentally obtained until now despite the fact that Ag_{44} is indeed a closed-shell structure,[3] and 4, 8, 12, 14, 16, and 20-electron structures of gold nanoclusters have also been reported,[2,4] see Table 1. The following questions have yet to be answered: Does the stable 18-electron shell closure structure of thiolated gold nanoclusters exist? If so, is the 18-electron shell closure structure more stable than the unclosed structure (e.g., 16-electron structure)? The recent finding of structural isomerism indicating the diversity of Au−Au bonding has also inspired us to study the aforementioned structures.[4n,r]

Table 1. Relationship between the Number of Au Atoms and the Shell Electron Count for the Structurally Resolved Gold Nanoclusters

no. of Au atoms	no. of thiolates	shell electron count
18	$14^{4l,q}$	4
20	16^{4j}	4
23	16^{4e}	8^{a}
24	20^{4i} or 16^{4g}	4 or 8
25	18^{2}	8^{a}
28	$20^{4f,r}$	8
30	18^{4h}	12
36	24^{4d}	12
38	$24^{4c,n}$	14
40	24^{4p}	16
44	28^{4s}	16
52	32^{4s}	20
102	44^{4a}	58
130	50^{4k}	80
133	$52^{4m,o}$	81

[a]The clusters bear −1 charge.

Herein, we report the synthesis and structure of an 18-electron closed-shell gold nanocluster, $Au_{44}(2,4\text{-DMBT})_{26}$ (2,4-DMBTH = 2,4-dimethylbenzenethiol), which has the same gold number but a different number of thiolates and kernel structures as $Au_{44}(TBBT)_{28}$ (TBBTH = 4-*tert*-butylbenzenelth-

Received: July 11, 2016
Published: August 4, 2016

DOI: 10.1021/jacs.6b07178
J. Am. Chem. Soc. 2016, 138, 10425−10428

iol) (see Figures S1−2).[4s] This structure reveals that the chirality of $Au_{44}(2,4\text{-DMBT})_{26}$ originates from the arrangement of both staples (bridging thiolates) on the gold kernel and a portion of the kernel atoms. The latter chirality origin has not been previously reported. Although $Au_{44}(2,4\text{-DMBT})_{26}$ bears an 18-electron shell closure, it is less thermostable than $Au_{44}(TBBT)_{28}$, and the gold in $Au_{44}(2,4\text{-DMBT})_{26}$ exhibits more a positive charge state than that in $Au_{44}(TBBT)_{28}$ as determined by X-ray photoelectron spectroscopy (XPS).

Synthesis of the $Au_{44}(2,4\text{-DMBT})_{26}$ nanocluster was performed by a two-step synthesis method with some modifications.[4c,d,f,k,m] Briefly, the precursors of the multisized $Au_x(2,4\text{-DMBT})_y$ clusters were first synthesized by reducing the Au(I)-(2,4-DMBT) complexes with $NaBH_4$. Then, the precursors were treated with excess 2,4-DMBTH at 40 °C for 20 h, and the title nanoclusters were isolated by preparative thin-layer chromatography (see SI for further experimental details). The single crystals of $Au_{44}(2,4\text{-DMBT})_{26}$ were formed by vapor diffusion of acetonitrile into the toluene solution of $Au_{44}(2,4\text{-DMBT})_{26}$ over 1 month.

The UV/vis/NIR spectrum of crystals dissolved in CH_2Cl_2 is shown in Figure 1A. There are five absorption bands centered at 331, 389, 442, 543, and 670 nm. Electrospray ionization mass spectrometry (ESI-MS) was applied to determine the exact formula of the as-prepared nanoclusters, as electrospray ionization is a much softer ionization technique than matrix-assisted laser desorption ionization.[3a,b,4m,5] One dominant peak centered at m/z 6250.3 is shown in Figure 1B, corresponding to $[Au_{44}(2,4\text{-DMBT})_{26} + 2Cs]^{2+}$ (deviation: 0.1 Da; CsOAc was added to assist the ionization of the nanoparticles). The calculated isotopic pattern agreed with the experimental isotopic pattern (see inset of Figure 1B); thus, it is readily concluded that the nanocluster composition is $Au_{44}(2,4\text{-DMBT})_{26}$, which was further supported by both thermogravimetric analysis (TGA) and XPS (see Figure 1C,D, respectively). The XPS analyses reveal that the Au/S atomic ratio is 43.4/26, which is consistent with the theoretical ratio of 44/26. The results of the TGA show a weight loss of 29.4 wt %, which is in perfect agreement with the theoretical value of $Au_{44}(2,4\text{-DMBT})_{26}$ (29.2 wt %). Furthermore, because XPS and TGA did not detect counterions, such as TOA^+, Cl^-, or Br^-, the possibility of anionic or cationic cases, i.e., $[Au_{44}(2,4\text{-DMBT})_{26}]^-$ or $[Au_{44}(2,4\text{-DMBT})_{26}]^+$, was excluded.

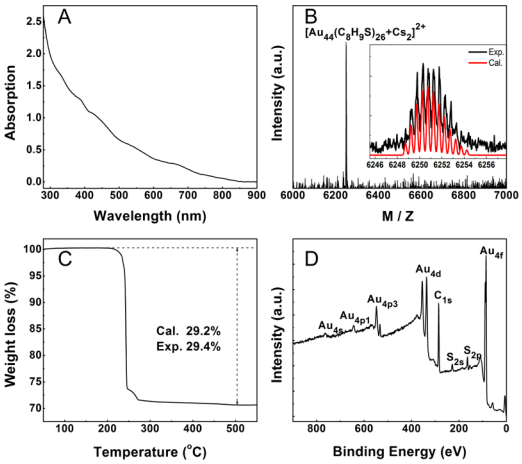

Figure 1. UV/vis/NIR absorption (A), ESI-MS (B), TGA (C), and XPS (D) results of $Au_{44}(2,4\text{-DMBT})_{26}$.

The composition was confirmed by single crystal X-ray crystallography (SCXC), which revealed that the crystal of $Au_{44}(2,4\text{-DMBT})_{26}$ adopts a triclinic space group of *P*-1, and the unit cell of the crystal contains a pair of enantiomeric nanoclusters (see Figure S2A). In contrast to $Au_{44}(TBBT)_{28}$, the $Au_{44}(2,4\text{-DMBT})_{26}$ nanocluster consists of an Au_{29} kernel capped by an exterior shell including two 2,4-DMBT thiolates, three $Au(2,4\text{-DMBT})_2$, and six $Au_2(2,4\text{-DMBT})_3$ staples (see Figure S2B). The Au_{29} kernel of $Au_{44}(2,4\text{-DMBT})_{26}$ is composed of a face-fused bi-icosahedral Au_{23}, as in Au_{38Q},[4c,n] and a special Au_6 bottom cap (see Figures 2A,F,G). One $Au(2,4\text{-DMBT})_2$ and four $Au_2(2,4\text{-DMBT})_3$ staples cap the Au_{23} (see Figure 2H,I), two $Au(2,4\text{-DMBT})_2$ and two $Au_2(2,4\text{-DMBT})_3$ staples bridge the Au_{23} and Au_6 bottom cap (see Figure 2J,K), and two 2,4-DMBT thiolates are located on the Au_6 surface. In the Au_{23} of $Au_{44}(2,4\text{-DMBT})_{26}$, the bond lengths between the central atom and the first shell Au atom range from 2.72 to 2.88 Å, whereas the Au−Au distance within the fusion plane is 3.10−3.20 Å. In the Au_6 bottom cap, the Au−Au distance is 2.74−3.20 Å. One of $Au(2,4\text{-DMBT})_2$ staples bridges one of the Au_6 corrugated planes by stapling the three farthest Au−Au pairs (5.48 Å), whereas the remaining

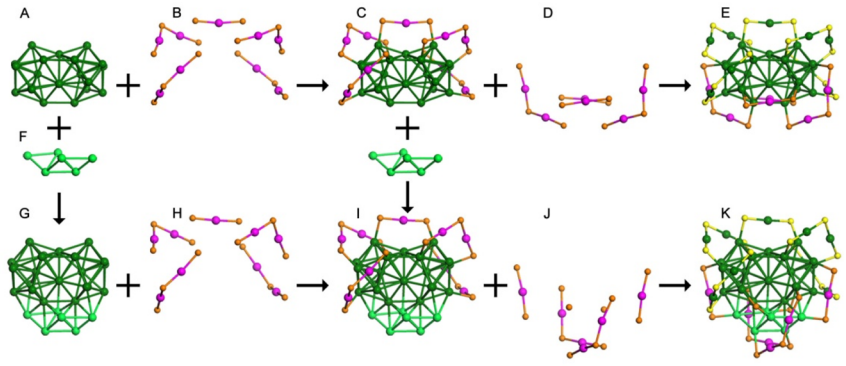

Figure 2. Anatomy of structures of Au_{38Q}[4c] and $Au_{44}(2,4\text{-DMBT})_{26}$ nanoclusters: Au_{23} kernel (A); four $Au_2(SCH_2CH_2Ph)_3$ and one $Au(SCH_2CH_2Ph)_2$ staples (B); $Au_{32}(2,4\text{-DMBT})_{14}$ framework (C); two $Au_2(SR)_3$ and two $Au(SR)_2$ staples (D); total structure of Au_{38Q} (E); Au_6 bottom cap (F); Au_{29} kernel (G); four $Au_2(2,4\text{-DMBT})_3$ and one $Au(2,4\text{-DMBT})_2$ staples (H); $Au_{38}(2,4\text{-DMBT})_{14}$ framework (I); two $Au_2(2,4\text{-DMBT})_3$, two $Au(2,4\text{-DMBT})_2$ staples, and two 2,4-DMBT thiolates (J); total structure of $Au_{44}(2,4\text{-DMBT})_{26}$ (K). For clarity, C and H are omitted. Color labels: yellow or orange = S; others = Au.

DOI: 10.1021/jacs.6b07178
J. Am. Chem. Soc. 2016, 138, 10425−10428

$Au(2,4\text{-DMBT})_2$ staples bridge Au_4 corrugated planes (which consists of an Au_3 from Au_{23} and one Au atom from the Au_6 bottom cap) by stapling the two farthest Au−Au pairs (5.09−5.27 Å) (see Figure 2C). The angle of S−Au−S stapling on the Au_6 plane is 175°, which is larger than that of S−Au−S stapling on the Au_4 corrugated plane (172°). The average Au−S−Au angle of the four $Au_2(2,4\text{-DMBT})_3$ on the surface of Au_{23} is ∼96.7°, which is smaller than that (∼105.5°) of the other two $Au_2(2,4\text{-DMBT})_3$ staples.

The other isomer of $Au_{44}(2,4\text{-DMBT})_{26}$ possesses the same Au_{23} unit, but the three monomeric staples, six dimeric staples, and Au_6 bottom cap rotate in different directions (see Figures 3). Therefore, the chirality of $Au_{44}(2,4\text{-DMBT})_{26}$ originates

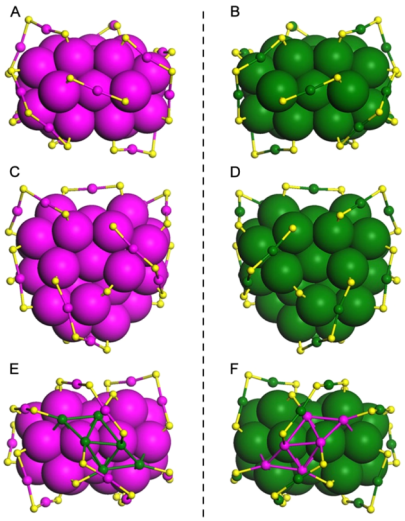

Figure 3. Two enantiomers of $Au_{44}(2,4\text{-DMBT})_{26}$ from different perspectives. Top (A, B), side (C, D), and bottom (E, F) views. For clarity, C and H are omitted. Color labels: yellow = S; olive or pink = Au.

from the arrangement of both the staples (bridging thiolates) and the Au_6 atoms. To the best of our knowledge, the finding that the chirality originates from part of the metal kernel has not been previously reported.[1c,4b,6] Although the kernel of $Au_{44}(TBBT)_{28}$ is achiral, $Au_{44}(TBBT)_{28}$ also exhibits chirality, which originates from the arrangement of the ligands.[4s] Furthermore, we have not observed any counterion in the unit cell of $Au_{44}(2,4\text{-DMBT})_{26}$, which further indicates that the title nanocluster is charge neural, which is consistent with the ESI-MS, TGA and XPS analyses.

The nominal shell closing electron count (n^*) for $Au_{44}(2,4\text{-DMBT})_{26}$ nanoclusters is 18 ($n^* = Nv_A - M - z = 44 \times 1 - 26 - 0 = 18$).[1a,7] As expected, the 18-electron closed-shell $Au_{44}(2,4\text{-DMBT})_{26}$ should be more stable than the 16-electron $Au_{44}(TBBT)_{28}$. However, it is found that $Au_{44}(2,4\text{-DMBT})_{26}$ is actually less thermostable than $Au_{44}(TBBT)_{28}$ under 80 °C, as monitored by UV/vis/NIR (see Figure 4), indicating that the thermostability of gold nanoclusters is not solely dependent on their electronic structure but is also influenced by some other factors such as protecting ligand,[4r] charge state[4t] and structure.[4c,n] $Au_{44}(2,4\text{-DMBT})_{26}$ and $Au_{44}(TBBT)_{28}$ have the same charge state and similar ligand, but distinctly different structure (non-fcc vs fcc, see Figures S1−2). The structural factor likely plays a more important role to the thermal stability compared with the electronic factor herein. The higher Au/S atomic ratio of $Au_{44}(2,4\text{-DMBT})_{26}$ in contrast to

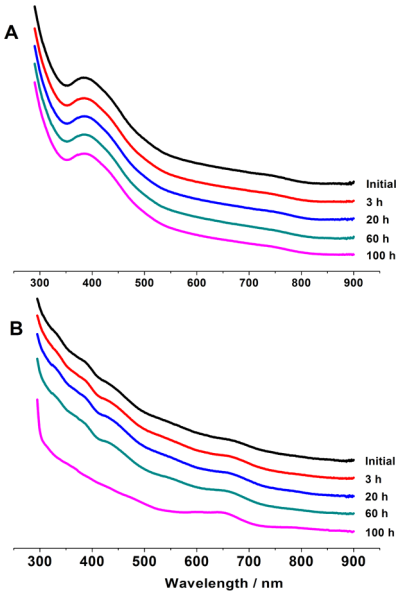

Figure 4. Thermostability of $Au_{44}(TBBT)_{28}$ (A) and $Au_{44}(2,4\text{-DMBT})_{26}$ (B) monitored by UV/vis/NIR spectroscopy.

$Au_{44}(TBBT)_{28}$ indicated that the charge state of gold in $Au_{44}(2,4\text{-DMBT})_{26}$ might be less positive than that in $Au_{44}(TBBT)_{28}$.[8] However, it is found that the Au 4f binding energies (88.6 eV for Au $4f_{5/2}$ and 84.9 eV for Au $4f_{7/2}$) of $Au_{44}(2,4\text{-DMBT})_{26}$ are distinctly higher than those of $Au_{44}(TBBT)_{28}$ (88.0 eV for Au $4f_{5/2}$ and 84.3 eV for Au $4f_{7/2}$) and even slightly higher than the Au 4f binding energies of the Au-(2,4-DMBT) complex (88.5 eV for Au $4f_{5/2}$ and 84.8 eV for Au $4f_{7/2}$), regardless of the fact that Au-TBBT and Au-(2,4-DMBT) complexes have very closed Au 4f binding energies (see Figure 5). The high Au 4f binding energies of

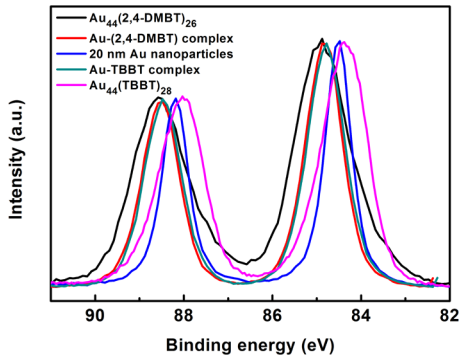

Figure 5. Au 4f XPS spectra of $Au_{44}(2,4\text{-DMBT})_{26}$, Au-(2,4-DMBT) complex, ∼20 nm Au nanoparticles, Au-TBBT complex, and $Au_{44}(TBBT)_{28}$.

$Au_{44}(2,4\text{-DMBT})_{26}$ were not expected nor have they been previously reported, indicating the variety of Au charge states in gold nanoclusters. One contribution to the high Au 4f binding energies of $Au_{44}(2,4\text{-DMBT})_{26}$ may be the high proportion of surface gold(I) of $Au_{44}(2,4\text{-DMBT})_{26}$ compared with that of $Au_{44}(TBBT)_{28}$, since the kernel (Au_{29}) of $Au_{44}(2,4\text{-DMBT})_{26}$ is smaller than the kernel (Au_{36}) of $Au_{44}(TBBT)_{28}$.[4s]

In summary, we have synthesized a novel 44-gold-atom nanocluster, the composition of which was determined to be $Au_{44}(2,4\text{-DMBT})_{26}$ by mass spectrometry, SCXC, XPS, TGA, etc. SCXC revealed that the structure consists of an Au_{29}

DOI: 10.1021/jacs.6b07178
J. Am. Chem. Soc. 2016, 138, 10425−10428

kernel, two 2,4-DMBT thiolates, three $Au(2,4\text{-DMBT})_2$, and six $Au_2(2,4\text{-DMBT})_3$ staples, which is completely different from the structure of $Au_{44}(TBBT)_{28}$. The arrangement of staples and thiolates on the Au_{29} kernel, as well as the arrangement of the Au_6 cap atoms, induces chirality in the $Au_{44}(2,4\text{-DMBT})_{26}$ nanoclusters. The latter chirality origin has not been previously reported. Our work demonstrates that the existence of gold nanoclusters with an 18-electron shell closure structure and the thermostability of gold nanoclusters are not solely determined by their electronic structure. Surprisingly, it was found that the Au 4f binding energies of $Au_{44}(2,4\text{-DMBT})_{26}$ are remarkably higher than those of $Au_{44}(TBBT)_{28}$ and even slightly higher than the Au 4f binding energies of Au-TBBT and Au-(2,4-DMBT) complexes, indicating that the charge state of Au in gold nanoclusters is not necessarily close to zero. The significance and novelty of this work lies in the following conclusions: (1) synthesis of a novel gold nanocluster $Au_{44}(2,4\text{-DMBT})_{26}$ and demonstration of the existence of an 18-electron shell closure structure; (2) determination of the atomic structure of $Au_{44}(2,4\text{-DMBT})_{26}$ by SCXC; (3) revealing that the chirality of gold nanoclusters could originate from the arrangement of partial kernel atoms; (4) finding that the 18-electron closed-shell structure may be less thermostable than the 16-electron structure, indicating that the stability of gold nanoclusters is influenced by multiple factors; and (5) discovering a variety of gold charge states in gold nanoclusters and demonstrating that the charge state of gold in gold nanoclusters could be even higher than that in Au-thiolate complexes.

■ ASSOCIATED CONTENT

Supporting Information

The Supporting Information is available free of charge on the ACS Publications website at DOI: 10.1021/jacs.6b07178.

Experimental details and data (PDF)
Crystallographic data for $Au_{44}(2,4\text{-DMBT})_{26}$ (CIF)

■ AUTHOR INFORMATION

Corresponding Author

*zkwu@issp.ac.cn

Author Contributions

‖These authors contributed equally.

Notes

The authors declare no competing financial interest.

■ ACKNOWLEDGMENTS

The authors would like to thank Natural Science Foundation of China (nos. 21222301, 21528303, 21171170), National Basic Research Program of China (grant no. 2013CB934302), the Ministry of Human Resources and Social Security of China, the Innovative Program of Development Foundation of Hefei Center for Physical Science and Technology (2014FXCX002), Hefei Science Center, CAS (user of potential: 2015HSC-UP003), the CAS/SAFEA International Partnership Program for Creative Research Teams and the Hundred Talents Program of the Chinese Academy of Sciences for financial support.

■ REFERENCES

(1) (a) Walter, M.; Akola, J.; Lopez-Acevedo, O.; Jadzinsky, P. D.; Calero, G.; Ackerson, C. J.; Whetten, R. L.; Groenbeck, H.; Hakkinen, H. *Proc. Natl. Acad. Sci. U. S. A.* **2008**, *105*, 9157. (b) Qian, H.; Zhu, M.; Wu, Z.; Jin, R. *Acc. Chem. Res.* **2012**, *45*, 1470. (c) Knoppe, S.; Buergi, T. *Acc. Chem. Res.* **2014**, *47*, 1318. (d) Mathew, A.; Pradeep, T. *Part. Part. Syst. Char.* **2014**, *31*, 1017.

(2) (a) Heaven, M. W.; Dass, A.; White, P. S.; Holt, K. M.; Murray, R. W. *J. Am. Chem. Soc.* **2008**, *130*, 3754. (b) Zhu, M.; Aikens, C. M.; Hollander, F. J.; Schatz, G. C.; Jin, R. *J. Am. Chem. Soc.* **2008**, *130*, 5883.

(3) (a) Harkness, K. M.; Tang, Y.; Dass, A.; Pan, J.; Kothalawala, N.; Reddy, V. J.; Cliffel, D. E.; Demeler, B.; Stellacci, F.; Bakr, O. M.; McLean, J. A. *Nanoscale* **2012**, *4*, 4269. (b) Desireddy, A.; Conn, B. E.; Guo, J.; Yoon, B.; Barnett, R. N.; Monahan, B. M.; Kirschbaum, K.; Griffith, W. P.; Whetten, R. L.; Landman, U.; Bigioni, T. P. *Nature* **2013**, *501*, 399. (c) Yang, H.; Wang, Y.; Huang, H.; Gell, L.; Lehtovaara, L.; Malola, S.; Hakkinen, H.; Zheng, N. *Nat. Commun.* **2013**, *4*, 2422.

(4) (a) Jadzinsky, P. D.; Calero, G.; Ackerson, C. J.; Bushnell, D. A.; Kornberg, R. D. *Science* **2007**, *318*, 430. (b) Pei, Y.; Gao, Y.; Zeng, X. C. *J. Am. Chem. Soc.* **2008**, *130*, 7830. (c) Qian, H.; Eckenhoff, W. T.; Zhu, Y.; Pintauer, T.; Jin, R. *J. Am. Chem. Soc.* **2010**, *132*, 8280. (d) Zeng, C.; Qian, H.; Li, T.; Li, G.; Rosi, N. L.; Yoon, B.; Barnett, R. N.; Whetten, R. L.; Landman, U.; Jin, R. *Angew. Chem., Int. Ed.* **2012**, *51*, 13114. (e) Das, A.; Li, T.; Nobusada, K.; Zeng, C.; Rosi, N. L.; Jin, R. *J. Am. Chem. Soc.* **2013**, *135*, 18264. (f) Zeng, C.; Li, T.; Das, A.; Rosi, N. L.; Jin, R. *J. Am. Chem. Soc.* **2013**, *135*, 10011. (g) Crasto, D.; Barcaro, G.; Stener, M.; Sementa, L.; Fortunelli, A.; Dass, A. *J. Am. Chem. Soc.* **2014**, *136*, 14933. (h) Crasto, D.; Malola, S.; Brosofsky, G.; Dass, A.; Hakkinen, H. *J. Am. Chem. Soc.* **2014**, *136*, 5000. (i) Das, A.; Li, T.; Li, G.; Nobusada, K.; Zeng, C.; Rosi, N. L.; Jin, R. *Nanoscale* **2014**, *6*, 6458. (j) Zeng, C.; Liu, C.; Chen, Y.; Rosi, N. L.; Jin, R. *J. Am. Chem. Soc.* **2014**, *136*, 11922. (k) Chen, Y.; Zeng, C.; Liu, C.; Kirschbaum, K.; Gayathri, C.; Gil, R. R.; Rosi, N. L.; Jin, R. *J. Am. Chem. Soc.* **2015**, *137*, 10076. (l) Das, A.; Liu, C.; Byun, H. Y.; Nobusada, K.; Zhao, S.; Rosi, N.; Jin, R. *Angew. Chem., Int. Ed.* **2015**, *54*, 3140. (m) Dass, A.; Theivendran, S.; Nimmala, P. R.; Kumara, C.; Jupally, V. R.; Fortunelli, A.; Sementa, L.; Barcaro, G.; Zuo, X.; Noll, B. C. *J. Am. Chem. Soc.* **2015**, *137*, 4610. (n) Tian, S.; Li, Y.-Z.; Li, M.-B.; Yuan, J.; Yang, J.; Wu, Z.; Jin, R. *Nat. Commun.* **2015**, *6*, 8667. (o) Zeng, C.; Chen, Y.; Kirschbaum, K.; Appavoo, K.; Sfeir, M. Y.; Jin, R. *Sci. Adv.* **2015**, *1*, e1500045. (p) Zeng, C.; Chen, Y.; Liu, C.; Nobusada, K.; Rosi, N. L.; Jin, R. *Sci. Adv.* **2015**, *1*, e1500425. (q) Chen, S.; Wang, S.; Zhong, J.; Song, Y.; Zhang, J.; Sheng, H.; Pei, Y.; Zhu, M. *Angew. Chem., Int. Ed.* **2015**, *54*, 3145. (r) Chen, Y.; Liu, C.; Tang, Q.; Zeng, C.; Higaki, T.; Das, A.; Jiang, D.-e.; Rosi, N. L.; Jin, R. *J. Am. Chem. Soc.* **2016**, *138*, 1482. (s) Zeng, C.; Chen, Y.; Iida, K.; Nobusada, K.; Kirschbaum, K.; Lambright, K. J.; Jin, R. *J. Am. Chem. Soc.* **2016**, *138*, 3950. (t) Zhu, M.; Eckenhoff, W. T.; Pintauer, T.; Jin, R. *J. Phys. Chem. C* **2008**, *112*, 14221.

(5) (a) Dass, A. *J. Am. Chem. Soc.* **2009**, *131*, 11666. (b) Fields-Zinna, C. A.; Sampson, J. S.; Crowe, M. C.; Tracy, J. B.; Parker, J. F.; deNey, A. M.; Muddiman, D. C.; Murray, R. W. *J. Am. Chem. Soc.* **2009**, *131*, 13844. (c) Wu, Z.; MacDonald; Mark, A.; Chen, J.; Zhang, P.; Jin, R. *J. Am. Chem. Soc.* **2011**, *133*, 9670. (d) Yuan, X.; Zhang, B.; Luo, Z.; Yao, Q.; Leong, D. T.; Yan, N.; Xie, J. *Angew. Chem., Int. Ed.* **2014**, *53*, 4623. (e) Joshi, C. P.; Bootharaju, M. S.; Alhilaly, M. J.; Bakr, O. M. *J. Am. Chem. Soc.* **2015**, *137*, 11578. (f) Negishi, Y.; Nakazaki, T.; Maloa, S.; Takano, S.; Niihori, Y.; Kurashige, W.; Yamazoe, S.; Tsukuda, T.; Hakkinen, H. *J. Am. Chem. Soc.* **2015**, *137*, 1206. (g) Zeng, J.-L.; Guan, Z.-J.; Du, Y.; Nan, Z.-A.; Lin, Y.-M.; Wang, Q.-M. *J. Am. Chem. Soc.* **2016**, *138*, 7848. (h) Luo, Z.; Nachammai, V.; Zhang, B.; Yan, N.; Leong, D. T.; Jiang, D.-e.; Xie, J. *J. Am. Chem. Soc.* **2014**, *136*, 10577.

(6) Tlahuice, A.; Garzon, I. L. *Phys. Chem. Chem. Phys.* **2012**, *14*, 7321.

(7) Wu, Z.; Jin, R. *Chem. - Eur. J.* **2011**, *17*, 13966.

(8) (a) Zhang, P.; Sham, T. K. *Phys. Rev. Lett.* **2003**, *90*, 245502. (b) Negishi, Y.; Nobusada, K.; Tsukuda, T. *J. Am. Chem. Soc.* **2005**, *127*, 5261.

DOI: 10.1021/jacs.6b07178
J. Am. Chem. Soc. 2016, 138, 10425−10428